DOI 10.31489/2022No2/75-85

UDC 621.311, 621.311.001.57

STUDY OF ALGORITHM SYNTHETIC INERTIA FUNCTIONING IN ELECTRIC NETWORKS OF DIFFERENT DENSITY

Rudnik V.E., Suvorov A.A., Razzhivin I.A., Ruban N.Yu., Andreev M.V.

National Research Tomsk Polytechnic University, Tomsk, Russia, ver3@tpu.ru

The ability to use the algorithm synthetic inertia (SI) is one of the most important properties of renewable energy sources (RES) generating units connected to the network via a power converter (GUPC). Through the use of SI algorithm there is an opportunity to increase the inertia and damping properties of such plants. The effectiveness of the SI algorithm depends on the mains frequency input value, which is formed by the phase locked loop (PLL), which is an integral part of the power converter control system. However, the operation of the PLL can lead to oscillations with different frequencies when the GUPC is installed in weak electrical networks and, accordingly, adversely affect the performance of the SI algorithm. The studies have shown that the PLL in the photovoltaic plant (PV) control system allows to influence the performance of the SI algorithm, but the nature of this influence depends on the electric network density and can be positive or negative. The influence obtained on the test EPS is also confirmed for the power system of large-scale.

Keywords: phase locked loop, synthetic inertia, photovoltaic plant, renewable energy sources, electric power system

Introduction

Currently, there is a trend of ever-increasing energy consumption. Many leading countries are interested in decarbonization, based on the reduction of traditional generation based on fossil fuels. One of the main directions of development of the global energy sector is the large-scale introduction of new generation facilities based on renewable energy sources (RES) [1]. According to the report of the International Energy Agency [2], the growth of installed RES capacity in 2020 was 280 GW, which is almost 45% more than in 2019, the record growth was also due to an increase of 23% of new photovoltaic installations of almost 135 GW of capacity.

Common to RES facilities is the use of power converters (PC) for connection to the network, which leads to the absence of direct coupling with the network and, accordingly, a contribution to the overall inertia of the system. The mentioned features of devices based on power semiconductor technology significantly change the dynamic properties of electric power systems (EPS) due to the different dynamics of PC functioning, especially its automatic control system (ACS), in comparison with traditional EPS equipment. As a result, the continuous growth of the implementation level of RES facilities, which will last until at least 2030 according to the Paris Agreement [3], leads to a significant decrease in the reliability of modern EPS functioning in normal and especially emergency modes [4-7].

One of the main problems is to ensure the frequency stability of EPS [8, 9]. The emergence of this problem is associated with the introduction of inertia-free RES facilities, including by replacing conventional generation, which leads to a decrease in the available power reserve and overall system inertia. This leads to an increase in the rate of voltage frequency change in the occurrence of power imbalance [10]. As a result, in power systems with low inertia, the depth of frequency reduction is much greater for a similar perturbation compared to traditional EPS [11, 12].

In order to ensure the reliable operation of EPS with low inertia and to reduce the negative effects from the implementation of RES facilities, it is necessary to adapt their ACS to the requirements of conventional generation as part of EPS [13]. Due to the necessary mass use of frequency control algorithms, developed solutions must be simple and reliable. Currently, many approaches have been developed to solve this problem and provide the formation of the so-called synthetic inertia. One such approach, which is applicable to all dominant types of RES, is the introduction of a synthetic inertia (SI) algorithm into the ACS, as well as

the correct tuning of the phase locked loop (PLL) [14-16]. The PLL is usually used to measure the network frequency, due to its simple structure and reliability, the PLL is the most popular and widely used [17].

In addition, during the operation of RES objects, it is necessary to take into account the heterogeneity of the magnitude of inertia, which leads to different rates of change and, accordingly, the values of frequency reduction in different parts of the network, which causes serious difficulties in setting up systems of protection against frequency reduction and increase. The problem of modeling transients in "weak" networks when implementing RES is worth mentioning separately [16, 18]. Due to the more oscillatory nature of transients in such networks, quite often there is a situation that after perturbations begin to oscillate with increasing amplitude, and also the PLL requires more fine-tuning, in contrast to networks with "strong" links [16]. In this paper [16, 18] it is shown that the coefficients of the PLL, especially in networks with "weak" links, strongly affect the operation of the power converter.

This paper deals with this issue and is organized as follows. First, the SI algorithm under consideration is described with the peculiarities of its application and the "underloading" mode of the photovoltaic plant (PV). Next, the mathematical model of the PV object used and the EPS test scheme are presented. The final section presents the results of the experiments with a corresponding description. The conclusions on the performed research are presented in the conclusion.

1. Approach to the implementation of the SI algorithm and the "deloading" mode PV

One of the main approaches to the formation of synthetic inertia is the use of SI [8, 15] Implementation of SI is usually considered in relation to wind turbines (WT) [8, 15, 19-21]. This is due to the possibility of using the stored energy of the rotating wind wheel for a short-term increase in the power output of the WT during the occurrence of frequency sag in the EPS. At the same time, there are 2 variants of implementation of the synthetic inertia algorithm: single-loop and double-loop control scheme (Figure 1). The double-circuit scheme has an obvious advantage over the single-circuit one [22] because it reacts not only in the process of frequency change, but also at the actual frequency deviation from the set value, thus providing a return to a higher frequency level after the occurrence of imbalance. Further we will consider the double-circuit circuit.

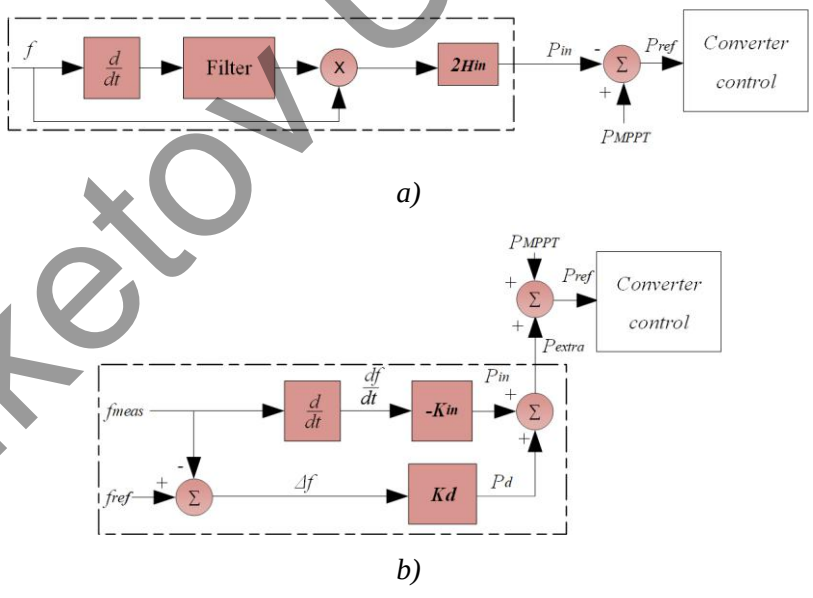

Fig. 1. Schematic diagram of the synthetic inertia algorithm: a) single-loop control, b) double-loop control

The double-loop circuit works as follows: when frequency fluctuations occur in the power system, the WT plant output power control system adds a Pextra frequency response signal to the active power setpoint. This signal is formed by a two-loop control circuit, including a frequency derivative control circuit df/dt and a frequency deviation circuit Δf. At the same time, the contribution in the formation of Pextra of the first loop is greatest in the initial stage of the transient process and does not imply the return of the network frequency to the nominal value. In order to ensure the return of frequency to the acceptable region, the second circuit is used, which imitates the effect of damped windings in a classical synchronous generator and provides linear frequency smoothing [23].

Application of PV for frequency control in emergency modes is possible in two ways. The first way is to use electric energy storage devices to deliver additional power, the second way is to "deloading" PV in steady-state mode and to use full power in emergency modes. In [24] it was proved that the first method has a higher cost, in this connection the widespread and currently main option is the "deloading" mode of PV. In this case, the use of synthetic inertia in the ACS PV allows the formation of an optimal frequency response and effective maintenance of stable operation of the EPS as a whole, including at different levels of illumination. Figure 2 shows the power dependence of the PV DC voltage. The Maximum Power Point Tracking (MPPT) controller normally changes the DC voltage of the panels to achieve maximum efficiency (point A1 in Figure 2).

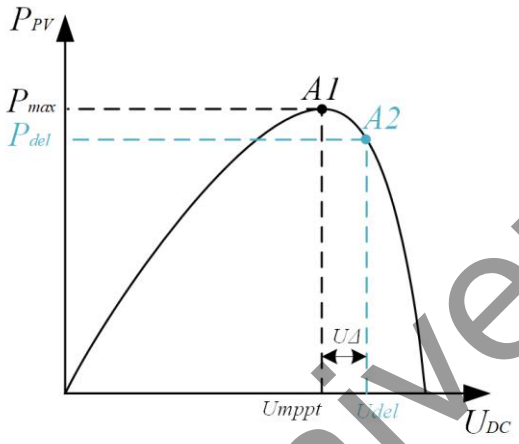

Fig. 2. Dependence of power on the DC voltage of the PV.

The Maximum Power Point and the corresponding DC voltage depend on solar insolation, ambient temperature, and solar cell temperature. There are many MPPT methods [25] to maximize PV power output. To unload the PV, the PV cell voltage is raised above the MPPT point by ΔU [26], the output power is reduced (point A2 in Figure 2) and a power reserve is created that can be used to provide inertial response and participate in frequency control. In view of the above, the research further uses a scheme that provides "deloading" of the PV and SI algorithm (Figure 3).

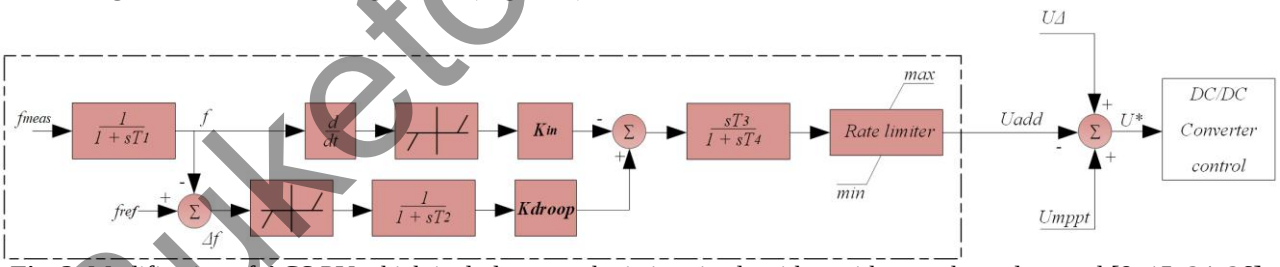

Fig. 3. Modification of ACS PV which includes a synthetic inertia algorithm with two-channel control [8, 15, 24, 26].

2. Description of test circuit EPS and the scheme of the PV used

For the research, a three-machine EPS was implemented as shown in Figure 4. The PV is implemented in bus 5 (Fig. 5), which is connected to the network by means of a static voltage converter (inverter). With a PV capacity of 25 MW, its share corresponds to 40% of the installed capacity. In the "deloading" mode of PV, there is a power reserve of 2.5 MW, which is 10% of the installed power [26]. For the presented network topology (Fig. 4), the following perturbation was carried out: load surge at busbar 3. The load surge allows to estimate the influence of the SI algorithm on the inertial response of the network.

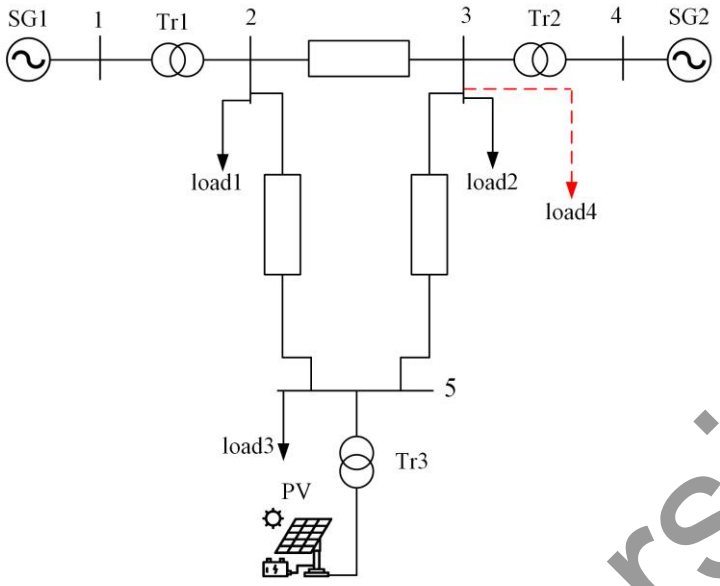

Fig. 4. Test three-machine power system.

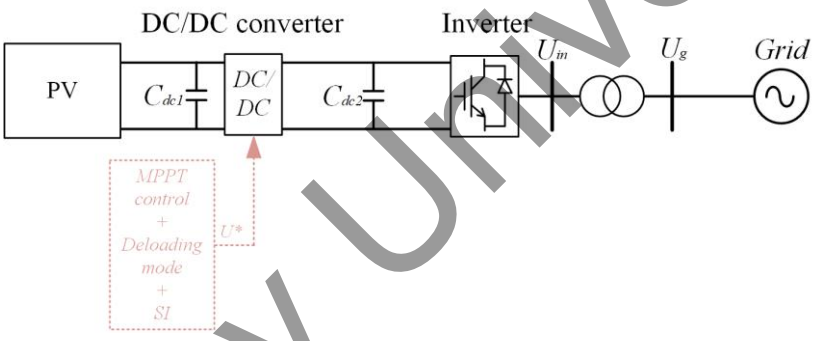

Fig. 5. Structural diagram of PV with upgraded ACS

To investigate the influence of the SI algorithm on the frequency stability, 2 variants of circuit-mode conditions are realized: "strong" and "weak" network. The strong network means that the short circuit ratio (SCR) of this network is more than 10 o.u. (SCR of "strong" network = 14,36), respectively SCR of weak network is less than 10 o.u. (SCR of "weak" network = 7,54) [27]. The calculation is made according to formula (1):

$$SCR = \frac{S_{\min}}{P_{RES}} \text{ [o.e.]}, \quad (1)$$

where, S_{min} - is the minimum value of short-circuit power at the RES connection point to the mains without RES influence, P_{RES} - is the rated power of RES.

3. Study of the influence of SI algorithm and PLL settings on EPS frequency stability

For the synthetic inertia algorithm (SI) coefficients were taken according to the analyzed literature: [28, 29] "Kin" differential coefficient we take equal to 2H (Kin=40) [28]. "Kdpoop" proportional coefficient is calculated according to the formula, relative to the network topology (2) [29].

$$Kdroop = \frac{Pg}{R} = 20 \text{ [p.u.]}, \quad (2)$$

where, Pg - power of PES (p.u.), R - equivalent droop coefficient of synchronous generators.

3.1 Study of the effect of the proportional and differential coefficient of the synthetic inertia algorithm on the stability of the power system by frequency.

Figure 6 and 7 show the oscillograms of frequency changes when varying the differential coefficient of the SI algorithm. From Fig. 6 and 7 we can see that increasing the differential coefficient leads to a decrease in the frequency sag, as is observed the damping of oscillations in both "strong" and "weak" network. The use of a larger differential coefficient has a positive effect on the transient process during load surge.

The proportional coefficient of the SI algorithm was varied in a similar way, the results are shown in Figures 8 and 9.

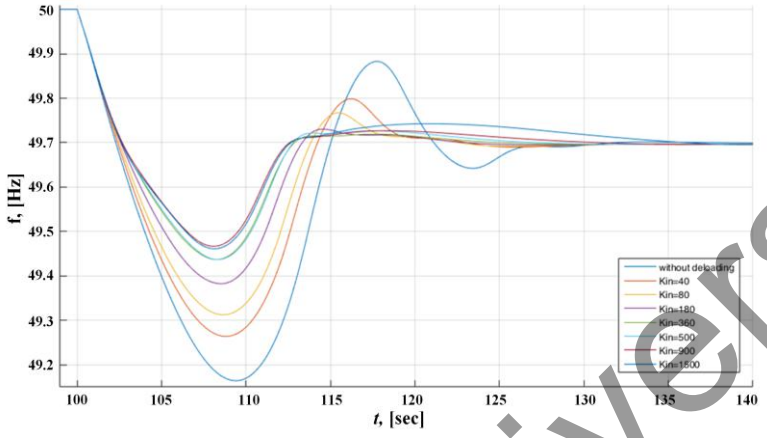

Fig. 6. Oscillograms of frequency changes when varying the "Kin" coefficient of the SI algorithm (Kdroop=const=20; SCR network = 14,36)

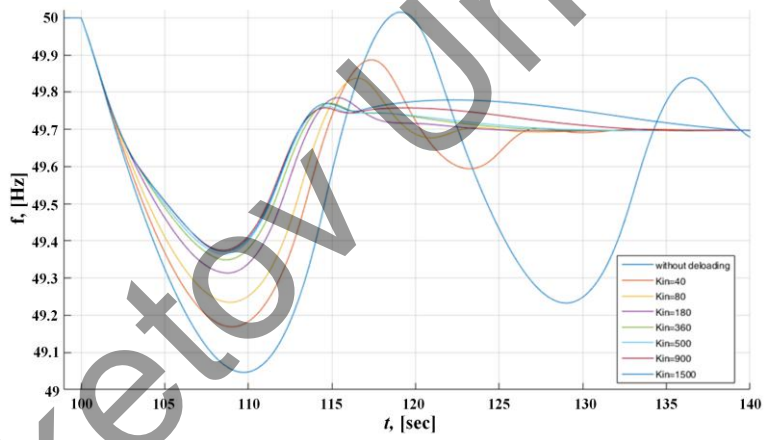

Fig. 7. Oscillograms of frequency changes when varying the "Kin" coefficient of the SI algorithm (Kdroop=const=20; SCR network = 7,54).

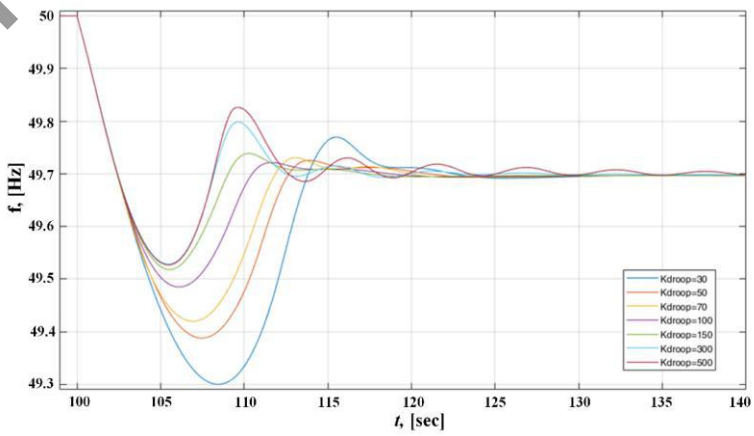

Fig. 8. Oscillograms of frequency changes when varying the coefficient "Kdroop" of the SI algorithm (Kin=const=40; SCR network = 14,36)

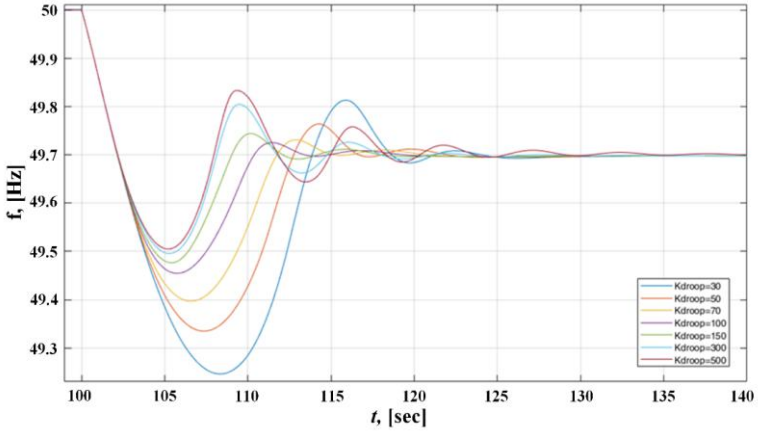

Fig. 9. Oscillograms of frequency changes when varying the coefficient "Kdroop" (Kin=const=40; SCR network = 7,54)

Figure 8 and 9 show that increasing the proportional coefficient leads to decreasing the frequency sag in both "strong" and "weak" networks. Increasing the proportional coefficient up to the value of 300 has a positive effect on the transient process in the "strong" network, a further increase in the coefficient leads to overshooting, which in turn leads to a decrease in network stability. This process has the same tendency for the "weak" network. Increasing the coefficients of the SI algorithm has a positive effect on the frequency stability of the EPS. However, the variation of coefficients should be within acceptable limits, in order to avoid a negative trend of frequency change, which can lead to an emergency situation and unstable state of EPS, respectively with the correct adjustment of the SI algorithm it is possible to maintain and improve the stability of EPS, which is confirmed by the obtained experimental results.

3.2. Study of the influence of the PLL bandwidth on the performance of the SI algorithm

As mentioned above, the study was conducted for "strong" and "weak" network, changing the PLL bandwidth in networks with different SCR led to different results. Calculation of the bandwidth of the PLL was performed according to [30]. The bandwidths for the studies were taken as follows: 0.3 Hz (Ki=0.83; Kp=1.2), 30 Hz (Ki=8390; Kp=130) and 50 Hz (Ki=20500; Kp=240) and SI algorithm coefficients were taken Kin=40; Kdpoop=20. Figures 10 and 11 show oscillograms of frequency changes and oscillograms of signal changes of SI algorithm at different PLL bandwidths in the "strong" and "weak" networks, respectively.

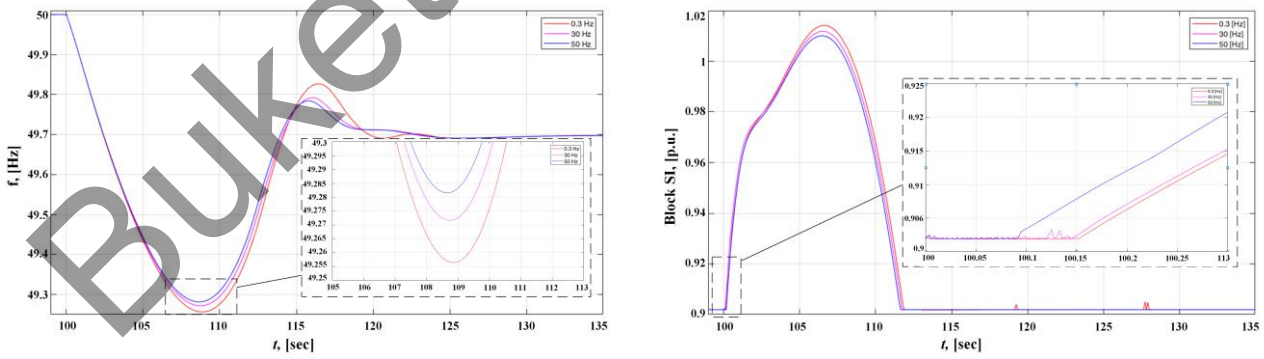

a *b*

Fig. 10. Oscillograms of the transient process in the "strong" network, where: a) frequency change at different bandwidth of the PLL, b) signal change of the SI algorithm at different bandwidth of the PLL

In a "strong" network, as the bandwidth of the PLL increases, the amount of frequency sag decreases (Figure 10a). This process occurs due to the fact that the PLL, with the entrainment of the bandwidth, increases the response speed of the SI algorithm (Figure 10b). In the "weak" network, the opposite picture is observed (Figure 11a), the PLL, with increasing bandwidth, decreases the response speed of the SI algorithm (Figure 11b), which leads to an increase in frequency droop.

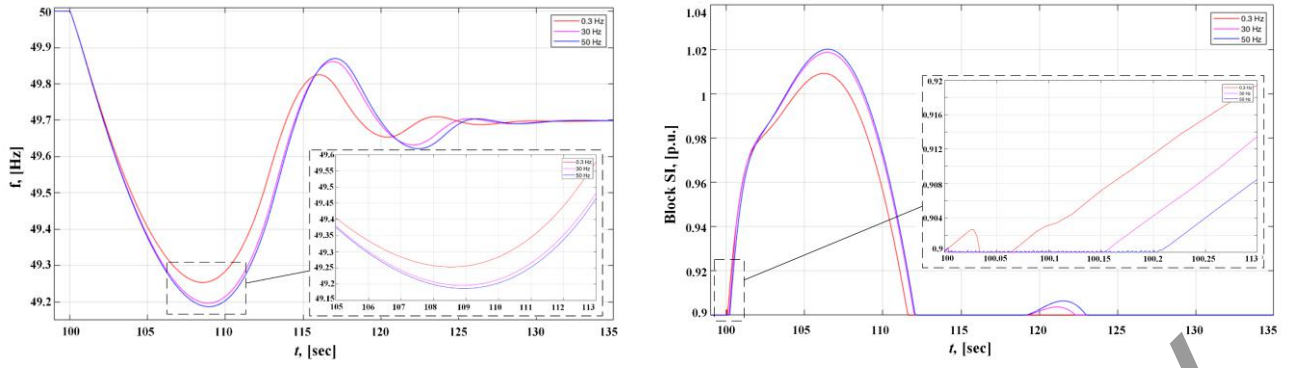

a *b*

Fig.11. Oscillograms of the transient process in the "weak" network, where: a) frequency change at different bandwidth of the PLL, b) signal change of the SI algorithm at different bandwidth of the PLL

Figures 12 and 13 show oscillograms of frequency changes and oscillograms of signal changes of SI algorithm on the differential channel when the "Ki" factor of the PLL increases in the "strong" network and "weak" network, respectively.

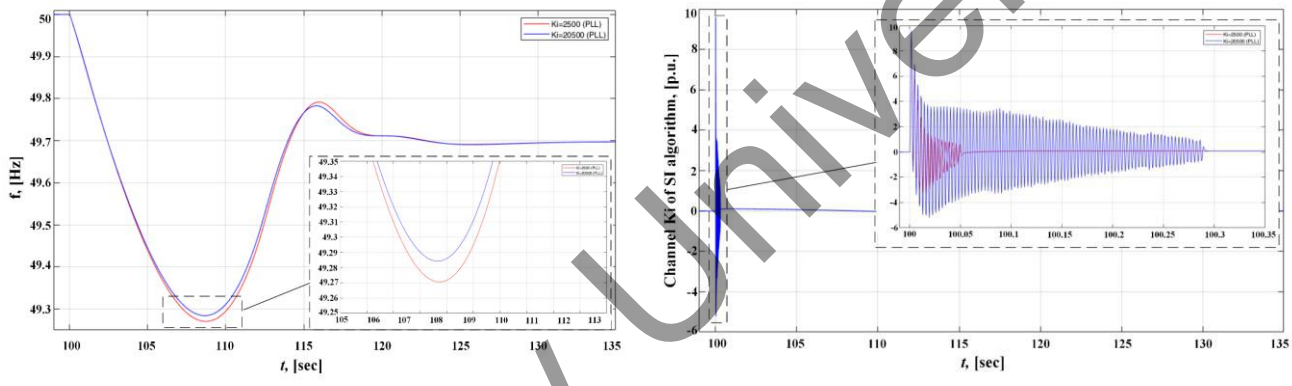

a *b*

Fig.12. Oscillograms of the transient process in the "strong" network, where: a) frequency change at different bandwidth of PLL, b) change of the SI algorithm signal on the differential channel when the "Ki" coefficient of the PLL increases

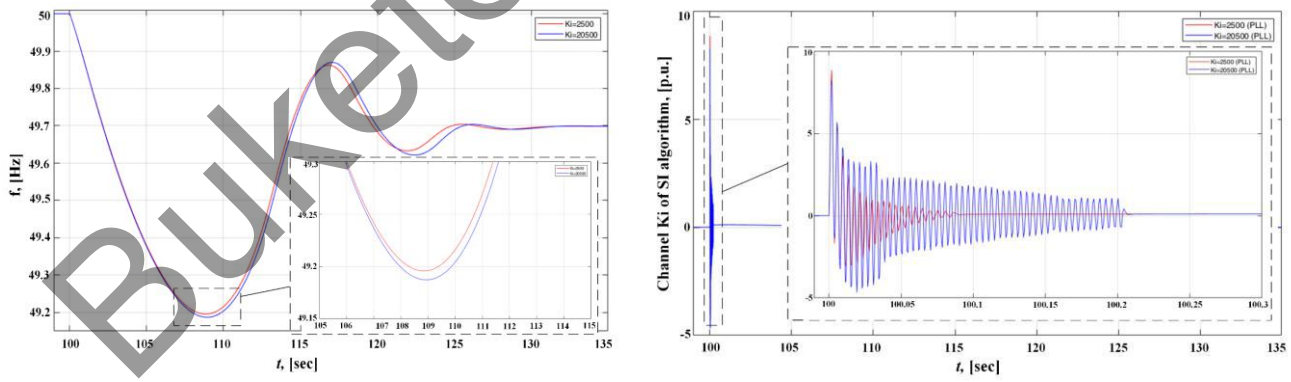

a *b*

Fig. 13. Oscillograms of the transient process in the "weak" network, where: a) frequency change at different bandwidth of PLL, b) change of the SI algorithm signal on the differential channel when the "Ki" coefficient of the PLL increases

At the moment of perturbation when the "Ki" coefficient of the PLL is larger, a signal of larger amplitude is generated in the differential channel of the SI algorithm (Fig. 12b), which leads to a smaller EPS frequency sag (Fig. 12a), in the "weak" network results in the opposite process (Figure 13 a, b). Figures 14 and 15 show oscillograms of frequency changes and oscillograms of signal changes of the SI algorithm on the differential channel when the "Kp" factor of the PLL increases in the "strong" and "weak" network, respectively.

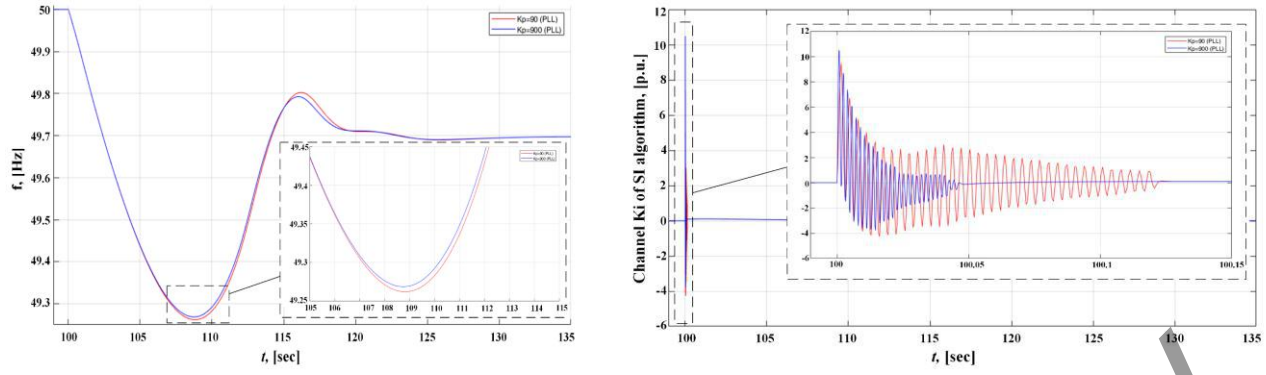

a *b*

Fig.14. Oscillograms of the transient process in the "strong" network, where: a) change of frequency at different bandwidth of PLL, b) change of signal of SI algorithm on differential channel when increasing the coefficient "Kp" of PLL

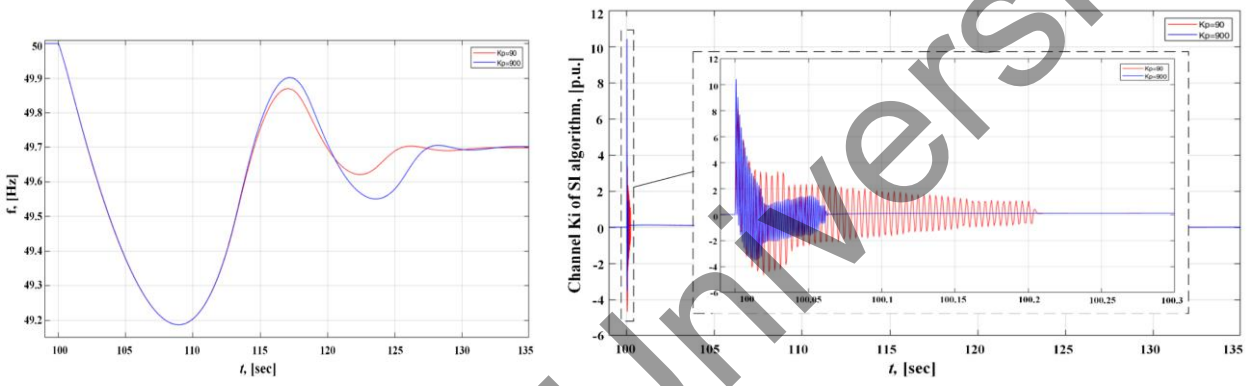

a *b*

Fig.15. Oscillograms of the transient process in the "weak" network, where: a) frequency change with different bandwidth of PLL, b) change of the SI algorithm signal on the differential channel when the "Kp" coefficient of the PLL increases

With the increase of "Kp" coefficient in the "strong" network, there is a positive tendency of frequency change: the level of frequency sag decreases (Figure 14a) due to the fact that the differential channel of SI algorithm generates a signal of larger amplitude (Figure 14b). With the increase of "Kp" coefficient in the "weak" network, the trend of frequency change has a negative character (Fig. 15a, b), there is an effect of overshoot on the second oscillation cycle, which is associated with the intensity of signal generation of differential channel of SI algorithm. Changing the settings of the PLL in the power converter control system allows to influence the characteristics of the frequency reduction process, but for the "strong" and "weak" network a different approach in setting is required.

3.3. A study of the effect of PLL bandwidth on the performance of an SI algorithm in a large-scale EPS

The study was conducted on a test power system of large-scale, which contains 177 bus (Figure 16). PV is being implemented in bus 176. The introduction of PV in this area is justified by suitable climatic conditions, the area is located near the zone of maximum intensity of solar radiation. The introduction of PV allows to solve the problems of the deficit energy district, and is one of the possible solutions to improve the reliability and sustainability of electricity supply. Also, this area is "weak" (SCR<10 o.u.), so in it is important to consider the identified patterns as in Section 4.2. To investigate the effect of the PLL bandwidth on the performance of the SI algorithm, load shedding at bus 170 was performed. The connection of the power district with the rest of the power system is carried out by a two-chain transmission line. The coefficients of the SI algorithm are calculated similarly to [28, 29], the bandwidths of the PLL are taken as in Section 4.2. Figure 17 shows the oscillograms of transients in the power system of large-scale.

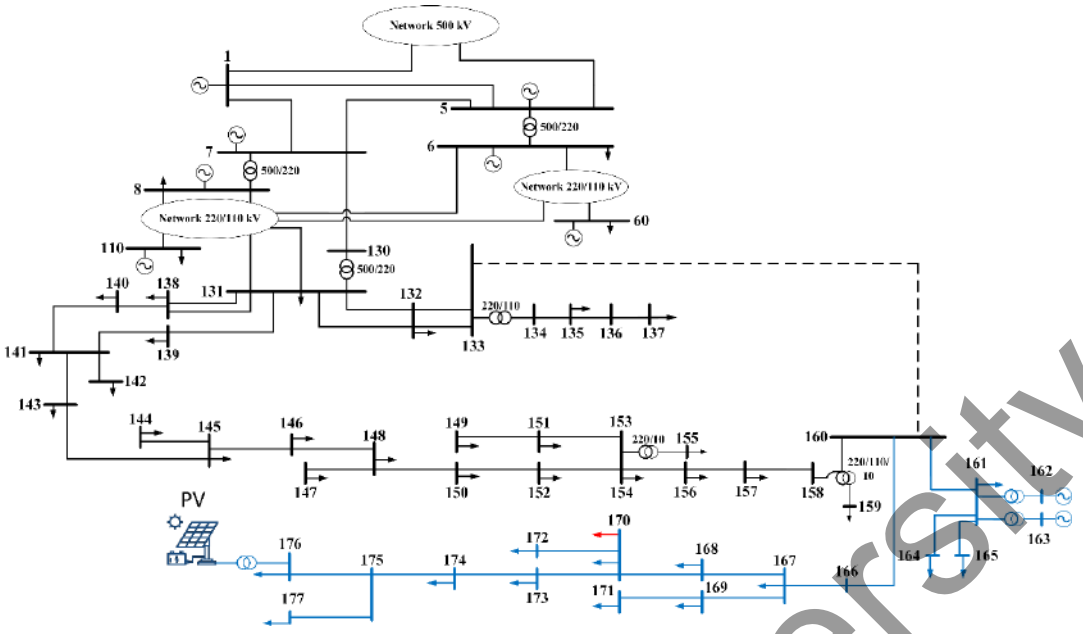

Fig. 16. Scheme of a large-scale EPS.

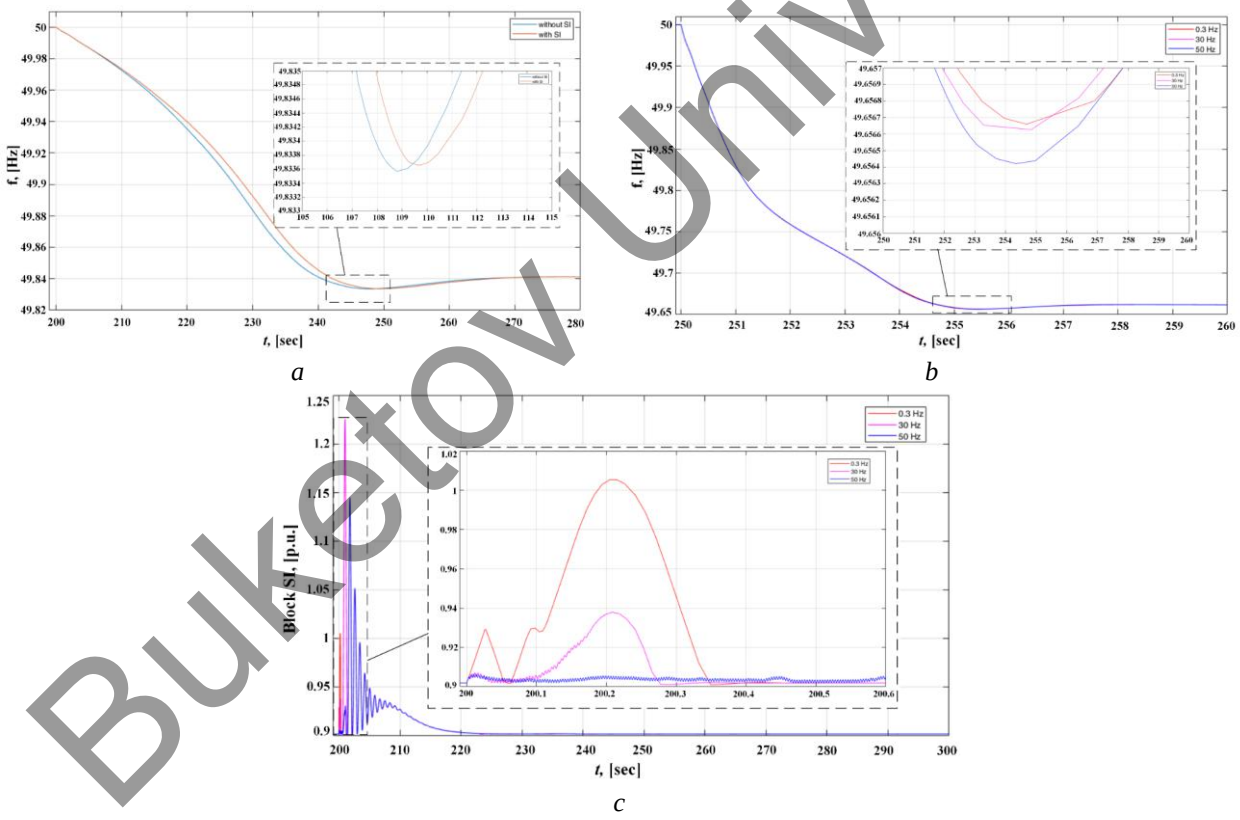

a *b* *c*

Fig. 17. Oscillograms of the transient process in the power system of large-scale where: a) frequency change in bus 176 when operating PV with and without SI algorithm; b) frequency change in bus 176 when varying the bandwidth of PLL; c) signal changes of SI algorithm when varying the bandwidth of PLL

Obviously, in large-scale EPS, the introduction of PV in general does not have a significant effect on the transients and does not dramatically reduce the overall inertia, but for a remote power district the contribution of PV including the SI algorithm and different setting of the PLL can have an impact on the transients. Figure 17a shows that the use of the SI algorithm has a positive effect on the frequency stability of the EPS, the frequency sag is reduced. Figure 17b shows that increasing the bandwidth PLL, leads to an

increase in the frequency sag in the EPS, this process occurs due to the fact that with increasing bandwidth PLL, decreases the response rate SI algorithm (Figure 17c). The regularities obtained in section 4.2. for the test EPS are also observed in large-scale EPS.

Conclusion

In the article the influence of SI algorithm on the frequency stability of EPS is investigated. It is noted that the correct adjustment of the SI algorithm has a significant impact on the dynamic stability of the network, especially in networks with a predominant fraction of RES. For the EPS test scheme, the results clearly show the possibility of a positive effect of SI algorithm on the dynamic stability of EPS. It is noted that varying the coefficients of the SI algorithm affects the transient process.

With a certain adjustment of the SI algorithm it is possible not only to provide the required inertial response, but also to extend the stability boundaries. It is also worth noting the effect of the PLL on the performance of the SI algorithm. The results show that changing the bandwidth of the PLL in the ACS PV allows to influence the process characteristics of both decreasing and increasing the frequency during the transient process, depending on the network topology. Accordingly, in a "strong" network, as the PLL bandwidth increases, the frequency sag decreases, while in a "weak" network, the opposite situation is observed. The same patterns obtained for the "weak" network in the test EPS are also observed in the high-dimensional EPS. The research proves that the problem of modeling transients in "weak" networks when implementing RES is relevant. Due to the more oscillatory nature of transients in such networks, quite often there is a situation that after perturbations begin to oscillate with increasing amplitude, and also the PLL requires more accurate tuning, in contrast to networks with "strong" links.

Acknowledgements

The reported study was funded by the Russian Science Foundation, project number 21-79-00129.

References

1 Wu J. Z., Yan J. Y., Jia H. J., Hatziargyriou N., Djilali N., Sun H. B. Integrated energy systems. *Applied Energy*, 2016, Vol. 167, pp. 155– 157. doi:10.1016/j.apenergy.2016.02.075

2 Renewable Energy Market Update 2021. Available at: https://www.iea.org/reports/renewable-energy-market-update-2021

3 OECD. World electricity generation by source of energy: Terawatt hours (TWh). Paris: OECD Publishing; 2016. // Available: https://doi.org/10.1787/factbook-2015-en

4 Sinsel, S. R., Riemke, R. L., Hoffmann, V. H. Challenges and solution technologies for the integration of variable renewable energy sources—a review. *Renewable Energy*, 2020, Vol. 145, pp. 2271 - 2285. https://doi.org/10.1016/j.renene.2019.06.147

5 National Grid, Voltage and Frequency Dependency. National Grid, 2018. Available: https://www.nationalgrid.com/sites/default/files/documents/SOFReport-Fr%ment.pdf

6 Huang S., Schmall J., Conto J., Adams J., Zhang Y., Carter C. "Voltage control challenges on weak grids with high penetration of wind generation: ERCOT experience." *IEEE Power and Energy Society General Meeting*, 2012, pp. 1-7. doi: 10.1109/PESGM.2012.6344713

7 Liu H., et al. Subsynchronous Interaction between Direct-Drive PMSG Based Wind Farms and Weak AC Networks. *IEEE Transactions on Power Systems*, 2017, Vol. 32, No. 6, pp. 4708-4720.

8 Cheng Y., Azizipanah-Abarghooee R., Azizi S., Ding L., Terzija V. Smart frequency control in low inertia energy systems based on frequency response techniques: A review. *Applied Energy*, 2020, vol. 279, 115798. https://doi.org/10.1016/j.apenergy.2020.115798.

9 JWG C2/C4.41: Impact of High Penetration of Inverter-based Generation on System Inertia of Networks. Available at: https://e-cigre.org/publication/wbn022-impact-of-high-penetration-of-inverter-based-generation-on-system

10 Johnson S.C, Rhodes J.D, Webber M.E. Understanding the impact of nonsynchronous wind and solar generation on grid stability and identifying mitigation pathways. *Applied Energy*, 2020, Vol. 262, pp. 114492.

11 Seneviratne, Chinthaka, Ozansoy C. Frequency response due to a large generator loss with the increasing penetration of wind/PV generation – A literature review. *Renewable and Sustainable Energy Reviews*, 2016, Vol. 57, pp. 659-668. DOI: 10.1016/j.rser.2015.12.051.

12 Razzhivin I., Askarov A., Rudnik V., Suvorov A. A Hybrid Simulation of Converter-Interfaced Generation as the Part of a Large-Scale Power System Model. *International Journal of Engineering and Technology Innovation*, 2021, Vol. 11, No. 4, pp. 278–293.

13 Arani M.F.M., El-Saadany E.F. Implementing virtual inertia in DFIG-based wind power generation. *IEEE Transactions on Power Systems*, 2013, Vol. 28, pp. 1373–84. https://doi.org/10.1109/TPWRS.2012.2207972

14 Zhong C, Zhou Y, Yan G. Power reserve control with real-time iterative estimation for pv system participation in frequency regulation. *International Journal of Electrical Power and Energy Systems*, 2021, Vol. 124, 106367. https://doi.org/10.1016/j.ijepes.2020.106367 .

15 Nguyen H. T., Yang G., Nielsen A. H., Jensen P. H. Frequency stability enhancement for low inertia systems using synthetic inertia of wind power. *IEEE Power and Energy Society General Meeting*, 2017, pp 1-5. doi: 10.1109/PESGM.2017.8274566

16 Qi Hu, Lijun Fu, Fa, Ma, Fen, Ji. Large Signal Synchronizing Instability of PLL-Based VSC Connected to Weak AC Grid. *IEEE Transactions on power systems*, 2019, Vol. 99. doi:10.1109/TPWRS.2019.2892224

17 Wan, Y. F., We, Li Y. Analysis and Digital Implementation of Cascaded Delayed-Signal-Cancellation PLL. *IEEE Transactions on Power Electronics*, 2011, Vol. 26, No. 4, pp. 1067-1080. doi: 10.1109/TPEL.2010.2091150

18 Zho, J Z., Ding H., Fan S., Zhang Y., Gole A.M. Impact of short-circuit ratio and phase-locked-loop parameters on the small-signal behavior of a VSC-HVDC converter. *IEEE Transactions on Power Delivery*, 2014, Vol.29, No. 5, pp. 2287–2296. doi: 10.1109/TPWRD.2014.2330518

19 Magnus D.M., et al. A novel approach for robust control design of hidden synthetic inertia for variable speed wind turbines. *Electric Power Systems Research*, 2021, Vol.196. doi:10.1016/j.epsr.2021.107267

20 Gutierrez F., Riquelme E., Barbosa K.A., Chavez H. State estimation for synthetic inertia control system using kalman filter. *Proceeding of the IEEE Intern. Conference on Automation 24th Congress of the Chilean Association of Automatic Control*, ICA-ACCA. 2021. doi:10.1109/ICAACCA51523.2021.9465316

21 Nguyen H.T., Chleirigh M.N., Yang G. A technical economic evaluation of inertial response from wind generators and synchronous condensers. *IEEE Access*, 2021, Vol. 9, pp.7183-7192.

22 Mohammad D, Mokhlis H., Mekhilef S. Inertia response and frequency control techniques for renewable energy sources: A review. *Renewable and Sustainable Energy Reviews*, 2017, Vol. 69, pp. 144-155. https://doi.org/10.1016/j.rser.2016.11.170

23 Bevran, H., Is, T., Miur, Y. Virtual synchronous generators: A survey and new perspectives. *International Journal of Electrical Power and Energy Systems*, 2014, Vol. 54, pp. 244-254. https://doi.org/10.1016/j.ijepes.2013.07.009

24 Zarina P.P., Mishra S., Sekhar P.C. Exploring frequency control capability of a PV system in a hybrid PV-rotating machine-without storage system. *International Journal of Electrical Power and Energy Systems*, 2014, Vol. 60, pp. 258-267. https://doi.org/10.1016/j.ijepes.2014.02.033

25 Karami N., Moubayed N., Outbib R. General review and classification of different MPPT techniques. *Renewable and Sustainable Energy Reviews*, 2017, Vol. 68, No. 1, pp. 1–18. https://doi.org/10.1016/j.rser.2016.09.132

26 Tielens P. *Operation and control of power systems with low synchronous inertia*. PhD diss. thesis, 2017.

27 Lingling Fan. Modeling Type-4 Wind in Weak Grids. *Proceeding of the IEEE Transactions on sustainable energy*, 2019, Vol.10, No. 2, pp. 853-864. doi: 10.1109/TSTE.2018.2849849

28 Zhang S., Jiao L., Zhang H., Shi L., Yang H. A new control strategy of active participation in frequency regulation of photovoltaic system. *Proceeding of the IEEE 4th Conference on Energy Internet and Energy System Integration: Connecting the Grids Towards a Low-Carbon High-Efficiency Energy System*, 2020, pp. 2314-2318. doi: 10.1109/EI250167.2020.9347015

29 Qiaoming Shi, Gang Wang, Weiming Ma, Lijun Fu, You Wu, Pengxiang Xing. Coordinated Virtual Inertia Control Strategy for D-PMSG Considering Frequency Regulation Ability. *Journal of Electrical Engineering and Technology*, 2016, Vol. 11, No. 6, pp. 1556-1570. http://dx.doi.org/10.5370/JEET.2016.11.6.1556

30 Sun Yin, (Erik) de Jong, E. C. W., Wang, Xiongfei, Yang, Dongsheng, Blaabjerg, Frede , Cuk, Vladimir, and (Sjef) Cobben, J. F. G. The Impact of PLL Dynamics on the Low Inertia Power Grid: A Case Study of Bonaire Island Power System. *Energies*, 2019, Vol. 12, No. 7, pp. 1259. https://doi.org/10.3390/en12071259.

Article accepted for publication 02.03.2022